

Storing a single photon as a spin wave entangled with a flying photon in the telecommunication bandwidth

Wei Zhang, Dong-Sheng Ding,^{*} Shuai Shi, Yan Li, Zhi-Yuan Zhou, Bao-Sen Shi,[†] and Guang-Can Guo

*Key Laboratory of Quantum Information, CAS, University of Science and Technology of China, Hefei, Anhui 230026, China
and Synergetic Innovation Center of Quantum Information & Quantum Physics, University of Science and Technology of China, Hefei, Anhui 230026, China*

(Received 13 September 2015; revised manuscript received 9 December 2015; published 11 February 2016)

Quantum memory is an essential building block for quantum communication and scalable linear quantum computation. Storing two-color entangled photons with one photon being at the telecommunication (telecom) wavelength while the other photon is compatible with quantum memory has great advantages toward the realization of the fiber-based long-distance quantum communication with the aid of quantum repeaters. Here, we report an experimental realization of storing a photon entangled with a telecom photon in polarization as an atomic spin wave in a cold atomic ensemble, thus establishing the entanglement between the telecom-band photon and the atomic-ensemble memory in a polarization degree of freedom. The reconstructed density matrix and the violation of the Clauser-Horne-Shimony-Holt inequality clearly show the preservation of quantum entanglement during storage. Our result is very promising for establishing a long-distance quantum network based on cold atomic ensembles.

DOI: [10.1103/PhysRevA.93.022316](https://doi.org/10.1103/PhysRevA.93.022316)

To realize a long-distance quantum communication, a quantum repeater has to be used to overcome the problem of communication fidelity decreasing exponentially with the channel length [1–3]. Quantum memories for light [4,5], which have been realized successfully during the past decade in many systems including a cold [6–11] or hot atomic system [12–15], a solid matter [16–18], a diamond [19], and others [20–22] are key components consisting of a quantum repeater. The realization of quantum repeaters requires the storage of quantum entanglement at local nodes and swapping the entanglement between adjacent nodes, which can be achieved by combining the two photons from different nodes intermediately [23–27]. Therefore, the photon traveling from the node to the location where Bell state measurement is performed in the low-loss window of an optical fiber is preferred. In this way, the number of repeaters could be reduced significantly. However this is very hard to realize in atomic media due to the lack of accessible energy levels in the scheme of Duan-Lukin-Cirac-Zoller (DLCZ) [1]. This problem can be overcome using two different solutions: One is the frequency conversion in atomic ensembles [28,29] or in nonlinear crystals [30] in which a three- or two-order nonlinear process has to be used. Another solution is to avoid this problem from the start by interfacing sources of entangled photons where one photon of each pair is at a telecommunication (telecom) wavelength with the other photon being compatible with an optical quantum memory [25,17,18] as pointed out in Ref. [5]. Kuzmich's group first established a quantum memory with telecom-wavelength conversion in 2010 [29] and later succeeded making it compatible for entanglement [28] in the DLCZ scheme using the frequency conversion method. However, an experimental realization of generating two-color entanglement in one atomic ensemble and storing this entangled photon in another ensemble as an atomic spin is reported here.

Here, we report the experimental storage of a two-color polarized entanglement in a cold atomic ensemble using the electromagnetically induced transparency (EIT) protocol by which the entanglement between the atomic spin wave and the photon in the telecom band is established. In our experiment, the polarization-entangled photons with the wavelength of one photon matching the transition wavelength of a rubidium (Rb) atom while the others being in telecom band are generated directly by spontaneously cascaded emission in one cold atomic ensemble, then this two-photon state is improved to be maximally entangled by letting one photon pass through a phase-insensitive Mach-Zehnder interferometer with an attenuation plate inside. After that, this photon is stored in another cold atomic ensemble embedded in the interferometer. In this way, the entanglement is established between the atomic ensemble and the telecom band photon which transmits in an optical fiber. After 100-ns storage, we convert the atom-photon entanglement to the photon-photon entanglement and check their entanglement. We reconstruct the density matrix for the photon-photon entanglement with a fidelity of $88.8\% \pm 4.4\%$ and obtain the violation of Clauser-Horne-Shimony-Holt (CHSH) inequality by a 3.2 standard deviation without any noise correction. All results clearly show the preservation of the entanglement during the storage. Our paper proves a successful quantum memory for two-color polarized entanglement in a cold atomic ensemble that constitutes a basis for building up a fiber-based long-distance quantum network.

Before showing our main results, we want to mention the fact that an erbium-crystal or an optical-crystal fiber can store a photon in the telecom band because these materials have suitable transition energy levels, however storing nonclassical light with a fidelity higher than the classical limit is a hard task in these materials due to improper relaxation dynamics for pumping [31] or noise issues [32]. Recently, Tittel's group demonstrated the storage and recall of an entangled 1532-nm-wavelength photon in an ensemble of cryogenically cooled erbium ions doped into a 20-m-long silica fiber using a photon-echo quantum-memory protocol [22].

^{*}Corresponding author: dds@ustc.edu.cn

[†]drshi@ustc.edu.cn

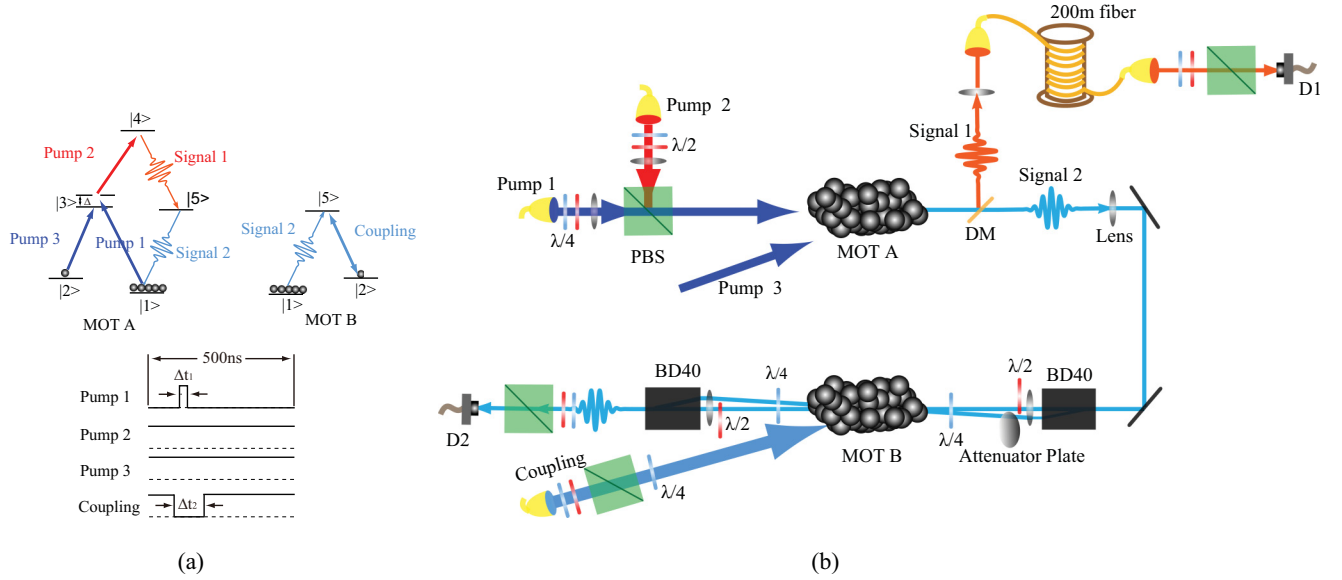


FIG. 1. (a) Simplified energy diagram and timing sequence for the generation of polarization entanglement. Pump 1 is a pulse of duration $\Delta t_1 = 20$ ns modulated by the acousto-optic modulator (AOM). Δt_2 represents the storage time. The single-photon detuning Δ is +130 MHz. $|1\rangle = |5S_{1/2}, F = 2\rangle$, $|2\rangle = |5S_{1/2}, F = 3\rangle$, $|3\rangle = |5P_{3/2}, F = 3\rangle$, $|4\rangle = |4D_{3/2}, F = 2\rangle$, $|5\rangle = |5P_{1/2}, F = 3\rangle$. (b) Simplified experimental setup. PBS: polarization beam splitter; $\lambda/2$ half-wave plate; $\lambda/4$ quarter-wave plate; D1: a free running In-GaAs single-photon detector (ID Quantique ID220-FR-SMF); D2: avalanche diode (PerkinElmer SPCM-AQR-15-FC); BD40: it can separate input light into two orthogonally polarized beams with 4.0-mm beam separation (Thorlabs BD40). The coupling light is above the two beams passing through BD40, and they both have 1.5° . The power of Pump 1, Pump 2, and the coupling light are 0.1, 8, and 20 mW, respectively.

The medium used here to generate a two-color polarization entangled photon pair is an optically thick ensemble of ^{85}Rb atoms trapped in a two-dimensional magneto-optical trap (MOT) [33]. The experimental setup is presented in Fig. 1. A pair of nonmaximally entangled photons with 795-nm ("Signal-2") and 1475-nm ("Signal-1") wavelengths, respectively, is created from the cold atomic ensemble in MOT A. To achieve this, 780-nm ("Pump-1") and 1530-nm ("Pump-2") lasers with orthogonal polarization collinearly pump the atomic ensemble under the condition of near two-photon resonance. Using a series of mirrors and lenses, the Signal-2 photon is delivered to the MOT B for subsequent storage, whereas the Signal-1 photon is coupled into a 200-m-long optical fiber. A self-locked Mach-Zehnder interferometer with two half-wave plates, two quarter-wave plates, and an attenuation plate used here has two important effects: One is to improve the entanglement of the photon pair, and the other is to guarantee the same memory efficiency for the differently polarized single-photon state, see Appendix B.

Our system works at the repetition rate of 100 Hz. A period of $T = 10$ ms includes the MOT trapping time (including initial state preparation) of $t_{\text{MOT}} = 8.7$ ms, and the operation time of $t_{\text{duty}} = 1.3$ ms, which contains 2600 cycles with a cycle time of 500 ns. During each cycle, Pump-2 and Pump-3 light beams are kept open, Pump 3 at a 780-nm wavelength is used to repump atoms in MOT A to the initial state $|1\rangle$. The Pump-1 light beam is shaped to be a pulse with 20-ns full width at half maximum (FWHM) every 500 ns. Both Pump-1 and Pump-2 light beams are focused on the atomic ensemble in MOT A with a focal length of 500 mm. Also, during the storage, Signal-2 photons are focused on the atomic ensemble in MOT B. The optical depths (ODs) of the atomic ensembles in MOT A and MOT B are 20 and 50, respectively.

Here the source is generated based on spontaneously four-wave mixing in atomic ensembles in which single atoms are pumped to state $|4\rangle$ through two-photon resonance, then back to state $|1\rangle$ with the emission of Signal 1 and Signal 2. The spontaneously four-wave mixings are widely used in diamond-type [34,35], ladder-type [36,37], and Λ -type [6] configurations in atomic media.

In this experiment, the nonmaximally two-color entangled photons, generated through spontaneously cascaded emission in a diamond-type configuration using orthogonal polarized pump light beams, can be expressed as a two-photon state [38],

$$|\psi_1\rangle = \cos \eta_f |H_{S_1} V_{S_2}\rangle + e^{i\phi_f} \sin \eta_f |V_{S_1} H_{S_2}\rangle, \quad (1)$$

where $|H_{S_1}\rangle$ ($|H_{S_2}\rangle$) and $|V_{S_1}\rangle$ ($|V_{S_2}\rangle$), respectively, represent the horizontal and vertical polarizations of Signal 1 (Signal 2). ϕ_f , a controllable parameter, represents the phase shifts induced by the pump light in the atomic media and the various optical elements. The mixing angle η_f , determined by the dipole matrix elements for different polarization, is very sensitive to the two-photon detuning of pump light, see Appendix A. In the experimental process, we find $\eta_f \approx 1.25\pi/4$ and $\phi_f \ll 1$ at -20 MHz of two-photon detuning. The photon pair is improved to be maximally entangled after the Signal-2 photon passes through a self-locked Mach-Zehnder interferometer with an attenuation plate inside, which is used to slightly attenuate the horizontal Signal-2 photon to balance two terms in the two-photon state. In this case, the two-photon state can be written as

$$|\psi_{\text{input}}\rangle = \frac{1}{\sqrt{2}} (|H_{S_1} V_{S_2}\rangle + |V_{S_1} H_{S_2}\rangle). \quad (2)$$

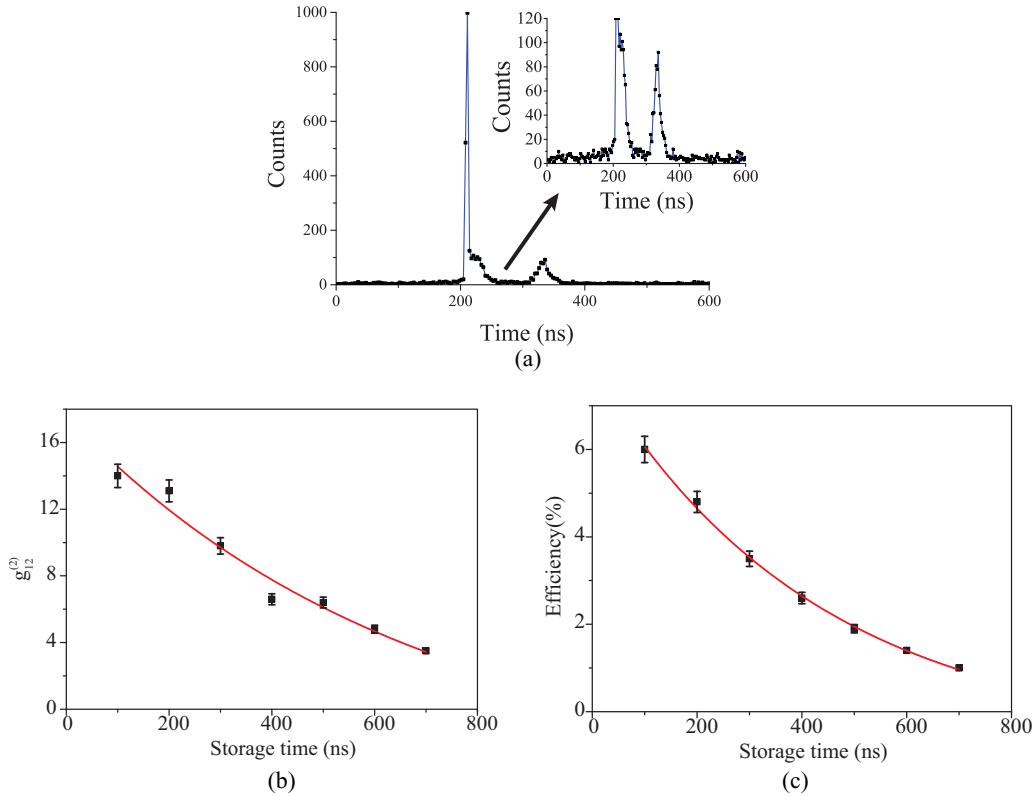


FIG. 2. Performance of the quantum memory. (a) Cross-correlation between Signal-1 and Signal-2 photons after 100-ns storage. (b) Cross-correlation $g_{12}^{(2)}$ versus storage time. (c) Storage efficiency versus storage time.

By this skill, the maximally entangled state was achieved between the Signal-2 photon and the Signal-1 photon transmitting in a 200-m-long optical fiber. Then we opened MOT B and stored the Signal-2 photon. Thus the entanglement was established between the collective atomic excitation (also called the spin wave) and the Signal-1 photon, which can be denoted as

$$|\psi_{as_i}\rangle = \frac{1}{\sqrt{2}}(|H_{S_1}V_a\rangle + |V_{S_1}H_a\rangle), \quad (3)$$

where $|H_a\rangle(|V_a\rangle)$ represents the collective atomic excitation.

Figure 2(a) shows the cross-correlation signal after 100-ns storage. And Figs. 2(b) and 2(c) described $g_{12}^{(2)}$ and storage efficiency decayed with the storage time. Experimentally, after a 100-ns storage, the collective atomic excitation in MOT B is read out to be a single photon. During this process, the storage time in MOT B should be shorter than the time delay of Signal 1 in the optical fiber in order to guarantee the storage of the entanglement. In our experiment, the time delay of the Signal-1 photon, determined by the transmission time in the optical fiber, is about $1 \mu\text{s}$. The storage efficiency for the programmed time of $\Delta t_2 = 100\text{ns}$ is $\sim 6\%$. To demonstrate experimentally whether the entanglement is preserved or not, individual projection measurements related to projecting the two-photon state into the four bases $|H\rangle, |V\rangle, (|H\rangle + |V\rangle)/\sqrt{2}$, and $(|H\rangle - i|V\rangle)/\sqrt{2}$ are performed on each photon before and after storing the 795-nm photon. According to the measurement results, we reconstructed the density

matrix of the photon pair before and after storage [39], which is shown in Fig. 3.

From the reconstructed density matrices, we calculate the fidelity which quantifies how closely the one state resembles the others. As is well known, the ideal retrieved polarized entangled state should be

$$|\psi_{\text{ideal}}\rangle = \frac{1}{\sqrt{2}}(|H_{S_1}V_{S'_2}\rangle + |V_{S_1}H_{S'_2}\rangle), \quad (4)$$

where $|H_{S'_2}\rangle$ denotes the photon retrieved from the atomic spin wave. The fidelity of the photon pair state before storage compared with the ideal state is $88.1\% \pm 2.6\%$ obtained by comparing the two-photon state density matrix ρ_{input} with the ideal density matrix ρ_{ideal} , using the formula $F_1 = \text{Tr}(\sqrt{\sqrt{\rho_{\text{input}}}\rho_{\text{ideal}}\sqrt{\rho_{\text{input}}}})^2$. Figure 3 depicts the real and imaginary parts of the density matrix for the state before and after storage. The storage fidelity $F_2 = \text{Tr}(\sqrt{\sqrt{\rho_{\text{output}}}\rho_{\text{input}}\sqrt{\rho_{\text{output}}}})^2$, which quantifies how closely the output state resembles the input state, is $88.8\% \pm 4.4\%$.

Furthermore, we demonstrate the entanglement after storage through checking the violation of the CHSH-type Bell inequality. We measure the correlation function $E(\theta_1, \theta_2)$, which can be calculated from each integration of the coincidence with $\theta_1(\theta_2)$ being the polarization angles of the half-wave plate for the Signal-1 (Signal-2) photon. We obtain the CHSH parameter $S = |E(\theta_1, \theta_2) - E(\theta_1, \theta'_2) + E(\theta'_1, \theta_2) + E(\theta'_1, \theta'_2)|$ with $\theta_1 = 0, \theta_2 = \pi/8, \theta'_1 = \pi/4$, and $\theta'_2 = 3\pi/8$. Here, the S values obtained are 2.49 ± 0.06 before storage and 2.38 ± 0.12 after 100-ns of storage without any noise correction.

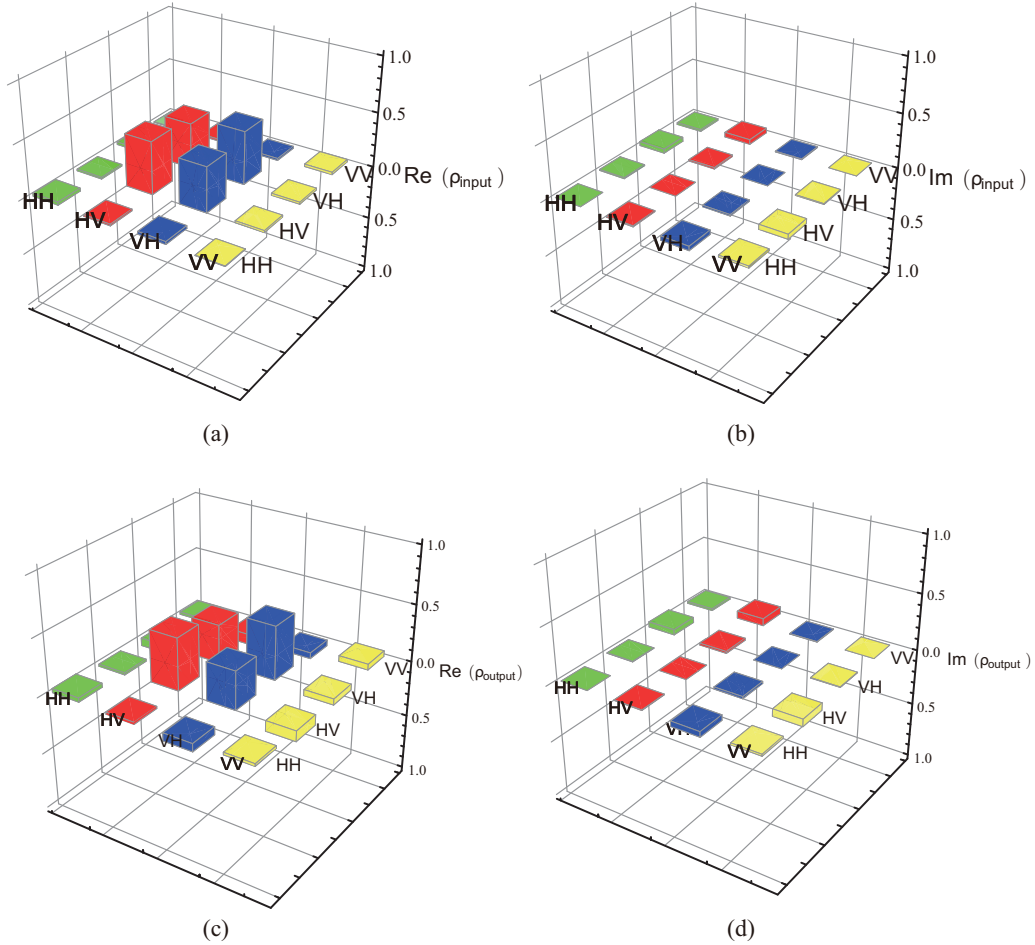


FIG. 3. (a) and (c) Real and (b) and (d) imaginary parts of the reconstructed density matrix of the two-photon state before (a) and (b) and after (c) and (d) storage, respectively, all data are raw without any noise correction.

We also study the two-photon interference in Fig. 4. We measure the coincidence counts while the Signal-1 photon is in the state $|H\rangle[(|H\rangle - |V\rangle)/\sqrt{2}]$ basis for varying polarization angles θ_2 of the half polarization plate for Signal 2 before and after storage. The results are given in Fig. 3. The fitted data showed the visibilities are $88.3\% \pm 2.7\%$ before and $81.2\% \pm 4.0\%$ after storage. Both values are larger than the threshold

of 70.7% and hence provide clear evidence of nonclassical interference, showing that entanglement is preserved.

In this experiment, the overall efficiency of storage is lower than 6% as depicted in Fig. 2(c). This is mainly due to the spectrum mismatch of Signal-2 photon with our memory system. The Signal-2 single photon has a broad spectrum band (100–200 MHz) which almost centers on the transition

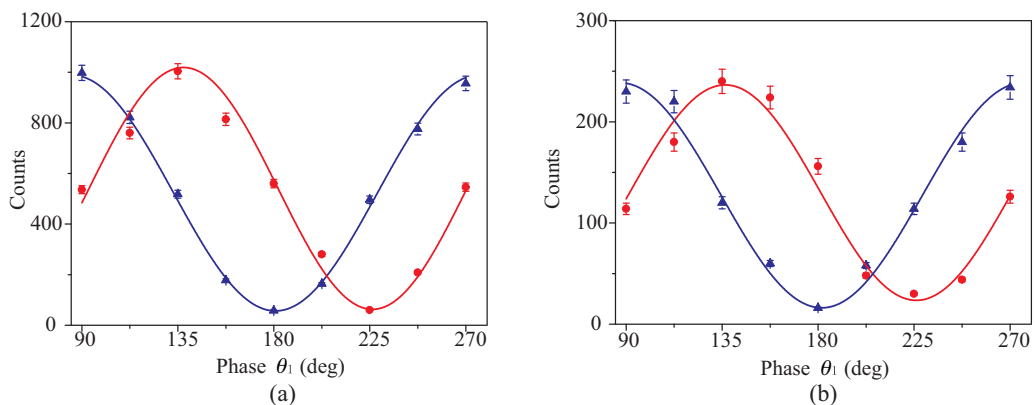


FIG. 4. (a) Two-photon interference before storage and (b) after storage. The blue (red) curve represents the coincidence rate with the Signal-1 photons projected onto state $|H\rangle[(|H\rangle - |V\rangle)/\sqrt{2}]$. The error bars are ± 1 standard deviation.

of $5S_{1/2}(F=2) \rightarrow 5P_{1/2}(F=3)$, measured by scanning a Fabry-Pérot cavity through temperature control. Usually, a broad bandwidth wave packet can be stored in the cold atomic system through Raman memory protocol, which requires a sufficient spectral separation from resonant transitions [10]. However, in our experiment, this broadband single-photon wave packet of Signal 2 is almost on resonance, which makes both EIT protocol and Raman protocol difficult to be effectively utilized. Finally, we take an improved-EIT protocol with carefully parameter adjustment and realize the storage with limited efficiency, see Appendix B.

Another important aspect is the noise issue. Due to the low memory efficiency of this process, the scattering noise coming from coupling laser has to be carefully eliminated. We use three homemade Fabry-Pérot cavities before detector D2 with a $10^7:1$ ratio and 40% transmission totally and a nearly backward coupling to reduce the scattering noise. The noise from Pump 1 (780 nm) is totally blocked by four 808-nm clean-up filters (Semrock LL01-808) with a 22° inclination. For 1475-nm single photons, we use three fiber gratings and a dichroic mirror (which are not depicted in Fig. 1) to avoid the Raman scattering generated by the coupling of the strong Pump 2 (1530 nm) into a 200-m-long fiber.

In general, memory time can be improved by compensating the magnetic field or by using magnetic-field-insensitive states and reducing atomic motion by using an optical lattice, and a millisecond or even hundred millisecond storage time could be achieved [40,41,29]. In addition, the dynamic decoupling method can also be used to improve the storage time [42]. Detection is mainly limited by the efficiency of the detector at the telecom wavelength, which is 10% with a $1\text{-}\mu\text{s}$ dead time here; hence, this experiment can be improved significantly if superconducting detectors can be used. A high-finesse cavity (~ 10 MHz) can be used to improve the memory process [9], and thereby high memory efficiency can be obtained.

To summarize, we have experimentally realized the preparation and storage of the two-color photonic polarization entanglement in which a 795-nm photon is stored in an atomic ensemble while a telecom-wavelength (1475-nm) photon transmits to a distant node by a 200-m-long fiber. Our work shows a basic memory element for future fiber-based long-distance quantum communication.

ACKNOWLEDGMENTS

This work was supported by the National Fundamental Research Program of China (Grant No. 2 011CBA00200) and the National Natural Science Foundation of China (Grants No. 11174271, No. 61275115, No. 61435011, and No. 61525504).

APPENDIX A: DETAILS ABOUT THE SOURCE

1. Coupling efficiency of Signal-1 and Signal-2 photons in details

The coupling efficiencies for two paths of Signal 2 are 75%. Signal-1 photons are collected through twice coupling: first from free space to fiber, then from free space to detector 1, with the coupling efficiencies of 82% and 80%, respectively. Before collected into a 200-m-long fiber, Signal 1 is filtered using a dichroic mirror (30 dB with 99% transmission,) and

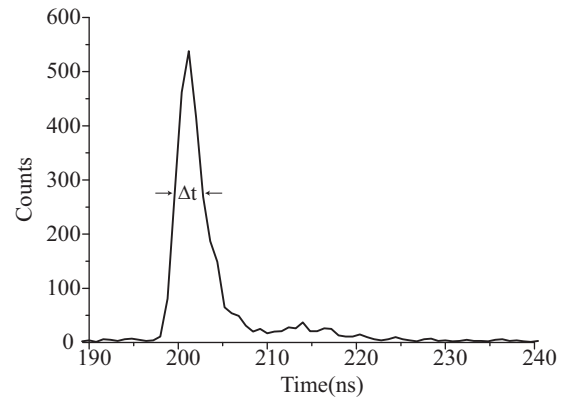


FIG. 5. Cross correlation between Signal-1 and Signal-2 photons without storage.

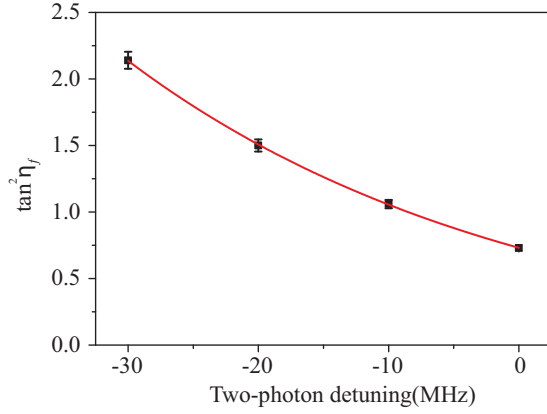
three fiber gratings (totally 90 dB with 95% transmission). In this way, the Raman scattering noise caused by Pump 2 coupled in the 200-m fiber is totally eliminated [here $X\text{dB} = 10 \log_{10}(\frac{\text{Signal 1 Transmission}}{\text{Pump 2 Transmission}})$]. Over all, the coupling efficiency of Signal 1 is around 60%.

2. Characterizing the nonclassical correlation between Signal-1 and Signal-2 photons

Figure 5 shows the coincidence counts between Signal 1 and Signal 2 before storage. Signal 1 and Signal 2 photons are nonclassically correlated in the time domain, which could be proved by checking whether the Cauchy-Schwarz inequality is violated or not. It is well known that classical light satisfies the inequality of $R = \frac{[g_{s1,s2}(\tau)]^2}{g_{s1,s1}(0)g_{s2,s2}(0)} \leq 1$. If $R > 1$, light is nonclassical where $g_{s1,s2}(\tau)$, $g_{s1,s1}(0)$, and $g_{s2,s2}(0)$ are the normalized second-order cross correlation and auto-correlation, respectively, of the photons. Before storage, we measured $g_{s1,s1}(0) = 1.2 \pm 0.1$, $g_{s2,s2}(0) = 1.38 \pm 0.12$, and $g_{s1,s2}(\tau) = 150 \pm 7$ at $\tau = 202$ ns. After 100-ns storage, we got $g_{s1,s1}(0) = 1.2 \pm 0.1$, $g_{s2,s2}(0) = 2$ [since the measured $g_{s2,s2}(0)$ after storage included autocorrelation of the leaked signal and autocorrelation of the retrieved signal, so the measured data did not represent the real autocorrelation of the stored signal. We took the fact that the retrieved photons exhibit photon statistics typical of thermal light], $g_{s1,s2}(\tau) = 14 \pm 0.7$ at $\tau = 325$ ns. So we got $R = 13587 \pm 3100$ before storage and $R = 82 \pm 14$ after 100-ns storage. Both were much larger than 1, the Cauchy-Schwarz inequality was strongly violated, clearly demonstrating the nonclassical correlation existed between Signal-1 and Signal-2 photons before and after storage.

3. Checking the single-photon properties of the Signal-2 photon

We also characterized the single-photon property of the Signal-2 photon by checking a heralded autocorrelation parameter α ($\alpha = \frac{P_{12}P_{123}}{P_{12}P_{13}}$, where P_1 was the Signal-1 photon counts, P_{12} and P_{13} are the twofold coincidence counts between the Signal-1 photon and the two separated Signal-2 photons by a beam splitter, P_{123} is the threefold coincidence counts), which was 0.04 ± 0.02 before storage and 0.3 ± 0.1


 FIG. 6. $\tan^2 \eta_f$ versus two-photon detuning.

after 100-ns storage. $\alpha < 0.5$ for Signal 2 before and after storage clearly demonstrated the single-photon nature.

4. Preparing a two-color entangled photon pair

Experimentally, we generated a two-color entangled photon pair via spontaneously cascaded emission in the cold atomic ensemble trapped in MOT A,

$$|\psi_1\rangle = \cos \eta_f |H_{S_1} V_{S_2}\rangle + e^{i\phi_f} \sin \eta_f |V_{S_1} H_{S_2}\rangle. \quad (\text{A1})$$

We found that the mixing angle η_f , determined by the dipole matrix elements for different polarizations, was very sensitive to the two-photon detuning of the pump lights. From the expression above we know $\tan^2 \eta_f$ represents the relative intensity of $V_{S_1} H_{S_2}$ to $H_{S_1} V_{S_2}$. We experimentally observed that $\tan^2 \eta_f$ was dependent on the two-photon detuning of the pump light as depicted in Fig. 6.

At the same time, with different two-photon detunings of the pump light, the time distribution of the generated Signal 2 (795 nm) was different. Figure 7 illustrated the experimental results where the time distribution of Signal 2 is obtained by a trigger which is synchronous with the Pump-1 pulse. The physical explanations of this phenomenon are not clear at present, which needs further investigation.

We can see from Fig. 7 that a small two-photon detuning of two pump lights makes the time distribution of the generated Signal-2 photon narrower. From Fig. 5, we know the FWHM of the two-photon wave packet is $\Delta t \approx 7$ ns, so the real single photon wave packet of Signal 2 is even narrower than 7 ns, so a narrower time distribution of the Signal-2 photon is preferred for efficient storage. Also considering the imbalance caused by two-photon detuning ($\tan^2 \eta_f$ relates to two-photon detuning, and $\tan^2 \eta_f = 1$ is the ideal parameter), we chose the detuning of -20 MHz as our experimental parameter. Under this condition, $\tan^2 \eta_f \sim 1.5$ and the FWHM of the time distribution of Signal 1 is about 50 ns.

APPENDIX B: MEMORY METHOD

1. Characterizing memory protocol: EIT protocol

We used a cavity (FWHM = 200 MHz) to determine the center frequency of Signal-2 photons and found it was near the resonance of the atomic transition $|1\rangle \rightarrow |5\rangle (|5S_{1/2} F=2\rangle \rightarrow |5P_{1/2} F=3\rangle)$. Then we used an improved-EIT protocol and successfully achieved the storage of this broad bandwidth and on-resonant single photon. Figure 8 illustrated the transmission spectra of a coherent 50- μ s probe light (black) versus probe detuning from the transition of $|1\rangle \rightarrow |5\rangle$ under the condition of absence (blue) and presence (red) of the coupling light with a power of 20 mW in an ensemble of MOT B. Here the probe light and

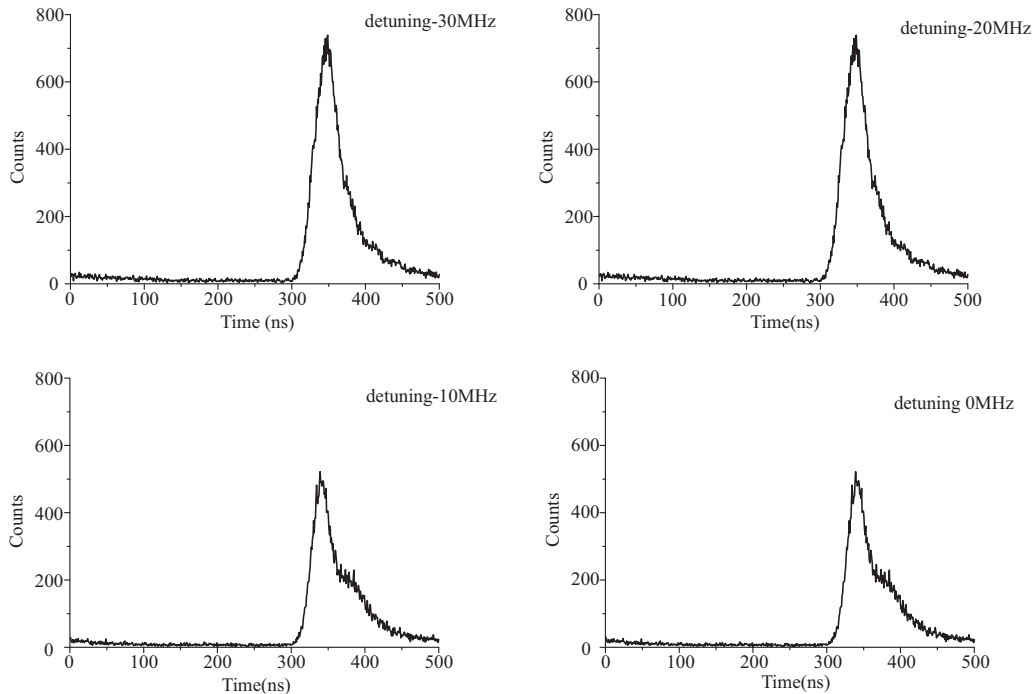


FIG. 7. Time distribution of Signal-2 versus two-photon detuning.

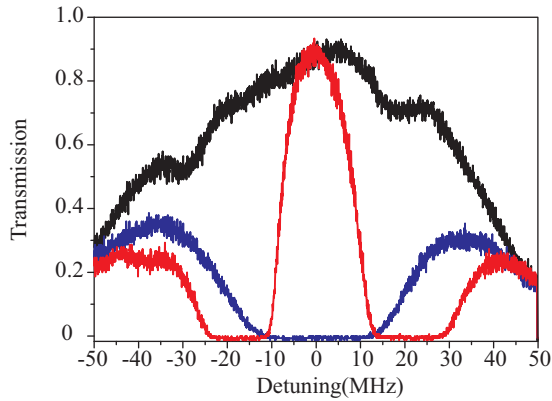


FIG. 8. Transmission spectra (blue) and EIT spectra (red). The black line is the 50- μ s probe light without an atomic ensemble in MOT B.

coupling light had σ^+ and σ^- polarizations. We wanted to emphasize that this $\sigma^+ - \sigma^-$ polarized (backward) configuration had broader and higher transmissions of the EIT window than that with the usual H - V polarized configuration. Here, we adopt a nearly backward operation of probe-coupling (178.5° angle between them) light to minimize the scatter noise. In addition, three homemade cavities were used to further filter

the scattering photons. The OD in MOT B was estimated to be ~ 50 . We observed a broad EIT window of 20 MHz.

2. The interferometer for storage

In the Mach-Zehnder interferometer shown in Fig. 1(b), we first used a half-wave plate on the path of vertical polarization after BD40, making the light in both paths have the same horizontal polarization. Then a quarter-wave plate was used to make the photon from any of the two paths have σ^+ polarization before entering MOT B. After leaving MOT B, another quarter-wave plate reverted its polarizations to be horizontal, followed by a half-wave plate in one path making the polarization of the photon in that path back vertical. This setup was intrinsically stable and without any locking circuit. Under this condition, we could accomplish the storage of an arbitrary state with the same efficiency. An attenuator here used was a balance for two terms in Eq. (1).

3. Error estimations

The error bars in the experimental data including CHSH and state tomography were estimated from Poisson statistics and using Monte Carlo simulations. The other error bars including the interference curves, $g_{12}^{(2)}$, and storage efficiency are from statistical measurements.

-
- [1] L.-M. Duan *et al.*, Long-distance quantum communication with atomic ensembles and linear optics, *Nature (London)* **414**, 413 (2001).
- [2] H.-J. Briegel, W. Dür, J. I. Cirac, and P. Zoller, Quantum Repeaters: The Role of Imperfect Local Operations in Quantum Communication, *Phys. Rev. Lett.* **81**, 5932 (1998).
- [3] H. J. Kimble, The quantum internet, *Nature (London)* **453**, 1023 (2008).
- [4] A. I. Lvovsky *et al.*, Optical quantum memory, *Nat. Photonics* **3**, 706 (2009).
- [5] F. Bussièrès *et al.*, Prospective applications of optical quantum memories, *J. Mod. Opt.* **60**, 1519 (2013).
- [6] A. Kuzmich *et al.*, Generation of nonclassical photon pairs for scalable quantum communication with atomic ensembles, *Nature (London)* **423**, 731 (2003).
- [7] C. Liu *et al.*, Observation of coherent optical information storage in an atomic medium using halted light pulses, *Nature (London)* **409**, 490 (2001).
- [8] T. Chanelière *et al.*, Storage and retrieval of single photons transmitted between remote quantum memories, *Nature (London)* **438**, 833 (2005).
- [9] H. J. Zhang *et al.*, Preparation and storage of frequency-uncorrelated entangled photons from cavity-enhanced spontaneous parametric down conversion, *Nat. Photonics* **5**, 628 (2011).
- [10] D.-S. Ding *et al.*, Raman quantum memory of photonic polarized entanglement, *Nat. Photonics* **9**, 332 (2015).
- [11] M. Lettner *et al.*, Remote Entanglement between a Single Atom and a Bose-Einstein Condensate, *Phys. Rev. Lett.* **106**, 210503 (2011).
- [12] C. H. van der Wal *et al.*, Atomic memory for correlated photon states, *Science* **301**, 196 (2003).
- [13] D. F. Phillips, A. Fleischhauer, A. Mair, R. L. Walsworth, and M. D. Lukin, Storage of Light in Atomic Vapor, *Phys. Rev. Lett.* **86**, 783 (2001).
- [14] K. F. Reim *et al.*, Toward high-speed optical quantum memories, *Nat. Photonics* **4**, 218 (2010).
- [15] K. F. Reim, P. Michelberger, K. C. Lee, J. Nunn, N. K. Langford, and I. A. Walmsley, Single-Photon-Level Quantum Memory at Room Temperature, *Phys. Rev. Lett.* **107**, 053603 (2011).
- [16] S. A. Moiseev *et al.*, Quantum memory photon echolike techniques in solids, *J. Opt. B: Quantum Semiclassical Optics* **5**, S497 (2003).
- [17] C. Clausen *et al.*, Quantum storage of photonic entanglement in a crystal, *Nature (London)* **469**, 508 (2011).
- [18] E. Saglamyurek *et al.*, Broadband waveguide quantum memory for entangled photons, *Nature (London)* **469**, 512 (2011).
- [19] D. G. England, P. J. Bustard, J. Nunn, R. Lausten, and B. J. Sussman, From Photons to Phonons and Back: A THz Optical Memory in Diamond, *Phys. Rev. Lett.* **111**, 243601 (2013).
- [20] P. J. Bustard, R. Lausten, D. G. England, and B. J. Sussman, Toward Quantum Processing in Molecules: A THz-Bandwidth Coherent Memory for Light, *Phys. Rev. Lett.* **111**, 083901 (2013).
- [21] M. R. Sprague *et al.*, Broadband single-photon-level memory in a hollow-core photonic crystal fibre, *Nat. Photonics* **8**, 287 (2014).
- [22] E. Saglamyurek *et al.*, Quantum storage of entangled telecom-wavelength photons in an erbium-doped optical fibre, *Nat. Photonics* **9**, 83 (2015).

- [23] N. Sangouard, C. Simon, H. de Riedmatten, and N. Gisin, Quantum repeaters based on atomic ensembles and linear optics, *Rev. Mod. Phys.* **83**, 33 (2011).
- [24] Y.-A. Chen *et al.*, Memory-built-in quantum teleportation with photonic and atomic qubits, *Nat. Phys.* **4**, 103 (2008).
- [25] C. Simon, H. de Riedmatten, M. Afzelius, N. Sangouard, H. Zbinden, and N. Gisin, Quantum Repeaters with Photon Pair Sources and Multimode Memories, *Phys. Rev. Lett.* **98**, 190503 (2007).
- [26] C. Nölleke, A. Neuzner, A. Reiserer, C. Hahn, G. Rempe, and S. Ritter, Efficient Teleportation Between Remote Single-Atom Quantum Memories, *Phys. Rev. Lett.* **110**, 140403 (2013).
- [27] F. Bussi eres *et al.*, Quantum teleportation from a telecom-wavelength photon to a solid-state quantum memory, *Nat. Photonics* **8**, 775 (2014).
- [28] Y. O. Dudin, A. G. Radnaev, R. Zhao, J. Z. Blumoff, T. A. B. Kennedy, and A. Kuzmich, Entanglement of Light-Shift Compensated Atomic Spin Waves with Telecom Light, *Phys. Rev. Lett.* **105**, 260502 (2010).
- [29] A. G. Radnaev *et al.*, A quantum memory with telecom-wavelength conversion, *Nat. Phys.* **6**, 894 (2010).
- [30] B. Albrecht *et al.*, A waveguide frequency converter connecting rubidium-based quantum memories to the telecom C-band, *Nature Communications* **5**, 3376 (2014).
- [31] B. Lauritzen, J. Min ar, H. de Riedmatten, M. Afzelius, N. Sangouard, C. Simon, and N. Gisin, Telecom-Wavelength Solid-State Memory at the Single Photon Level, *Phys. Rev. Lett.* **104**, 080502 (2010).
- [32] J. Dajczgewand *et al.*, Large efficiency at telecom wavelength for optical quantum memories, *Opt. Lett.* **39**, 2711 (2014).
- [33] Y. Liu *et al.*, Realization of a two-dimensional magneto-optical trap with a high optical depth, *Chin. Phys. Lett.* **29**, 024205 (2012).
- [34] B. Srivathsan, G. K. Gulati, B. Chng, G. Maslennikov, D. Matsukevich, and C. Kurtsiefer, Narrow Band Source of Transform-Limited Photon Pairs via Four-Wave Mixing in a Cold Atomic Ensemble, *Phys. Rev. Lett.* **111**, 123602 (2013).
- [35] T. Chaneli ere, D. N. Matsukevich, S. D. Jenkins, T. A. B. Kennedy, M. S. Chapman, and A. Kuzmich, Quantum Telecommunication Based on Atomic Cascade Transitions, *Phys. Rev. Lett.* **96**, 093604 (2006).
- [36] Z. Wei *et al.*, Non-classical correlated photon pairs generation via cascade transition of $5S_{1/2} - 5P_{3/2} - 5D_{5/2}$ in a hot ^{85}Rb atomic vapor, *Chin. Phys. Lett.* **31**, 064208 (2014).
- [37] D.-S. Ding *et al.*, Generation of non-classical correlated photon pairs via a ladder-type atomic configuration: theory and experiment, *Opt. Express* **20**, 11433 (2012).
- [38] D. N. Matsukevich, T. Chaneli ere, S. D. Jenkins, S.-Y. Lan, T. A. B. Kennedy, and A. Kuzmich, Entanglement of Remote Atomic Qubits, *Phys. Rev. Lett.* **96**, 030405 (2006).
- [39] D. F. V. James, P. G. Kwiat, W. J. Munro, and A. G. White, Measurement of qubits, *Phys. Rev. A* **64**, 052312 (2001).
- [40] B. Zhao *et al.*, A millisecond quantum memory for scalable quantum networks, *Nat. Phys.* **5**, 95 (2009).
- [41] Z. X. Xu, Y. Wu, L. Tian, L. Chen, Z. Zhang, Z. Yan, S. Li, H. Wang, C. Xie, and K. Peng, Long Lifetime and High-Fidelity Quantum Memory of Photonic Polarization Qubit by Lifting Zeeman Degeneracy, *Phys. Rev. Lett.* **111**, 240503 (2013).
- [42] G. Heinze, C. Hubrich, and T. Halfmann, Stopped Light and Image Storage by Electromagnetically Induced Transparency up to the Regime of One Minute, *Phys. Rev. Lett.* **111**, 033601 (2013).